The uremic toxin indoxyl sulfate interferes with iron metabolism by regulating hepcidin in chronic kidney disease

Hirofumi Hamano[1,2*], Yasumasa Ikeda[1*], Hiroaki Watanabe[3*], Yuya Horinouchi[1], Yuki Izawa-Ishizawa[1], Masaki Imanishi[2], Yoshito Zamami[2,3], Kenshi Takechi[4], Licht Miyamoto[5], Keisuke Ishizawa[2,3], Koichiro Tsuchiya[5], Toshiaki Tamaki[1]

[1]Department of Pharmacology, Institute of Biomedical Sciences, Tokushima University Graduate School, Tokushima, Japan

[2]Department of Pharmacy, Tokushima University Hospital, Tokushima, Japan

[3]Department of Clinical Pharmacy, Institute of Biomedical Sciences, Tokushima University Graduate School, Tokushima, Japan

[4]Clinical Trial Center for Developmental Therapeutics, Tokushima University Hospital

[5]Department of Medical Pharmacology, Institute of Biomedical Sciences, Tokushima University Graduate School, Tokushima, Japan

*These authors contributed equally to this work.

Corresponding author: Yasumasa Ikeda, MD, PhD

Department of Pharmacology, Institute of Biomedical Sciences,

Tokushima University Graduate School,

3-18-15 Kuramoto-cho, Tokushima, 770-8503, Japan

E-mail: yasuike@tokushima-u.ac.jp

Tel: +81-88-633-7061, Fax: +81-88-633-7062

Abstract

Background: Hepcidin secreted by hepatocytes is a key regulator of iron metabolism throughout the body. Hepcidin concentrations are increased in chronic kidney disease (CKD), contributing to abnormalities in iron metabolism. Levels of indoxyl sulfate (IS), a uremic toxin, are also elevated in CKD. However, the effect of IS accumulation on iron metabolism remains unclear.

Methods: We used HepG2 cells to determine the mechanism by which IS regulates hepcidin concentrations. We also used a mouse model of adenine-induced CKD. The CKD mice were divided into two groups: one was treated using AST-120 and the other received no treatment. We examined control mice, CKD mice, CKD mice treated using AST-120, and mice treated with IS via drinking water.

Results: In the *in vitro* experiments using HepG2 cells, IS increased hepcidin expression in a dose-dependent manner. Silencing of the aryl hydrocarbon receptor (AhR) inhibited IS-induced hepcidin expression. Furthermore, IS induced oxidative stress, and antioxidant drugs diminished IS-induced hepcidin expression. Adenine-induced CKD mice demonstrated an increase in hepcidin concentrations; this increase was reduced by AST-120, an oral adsorbent of the uremic toxin. CKD mice showed renal anemia, decreased plasma iron concentration, increased plasma ferritin, and increased iron content in the spleen. Ferroportin was decreased in the duodenum and increased in the spleen. These changes were ameliorated by AST-120 treatment. Mice treated by direct IS administration showed hepatic hepcidin upregulation.

Conclusion: IS affects iron metabolism in CKD by participating in hepcidin regulation via pathways that depend on AhR and oxidative stress.

Keywords: Indoxyl sulfate, hepcidin, iron, CKD, anemia

Running Head

Effect of indoxyl sulfate on hepcidin regulation

Short summary

In contrast with absolute iron deficiency, functional iron deficiency is common, and it causes renal anemia in chronic kidney disease. In the present study, we found that indoxyl sulfate (IS)—a uremic toxin—contributes to renal anemia by regulating hepcidin concentrations and thus impairing iron absorption and causing ectopic iron accumulation. This study presents the first findings regarding the effect of IS on hepcidin concentrations and thus on whole-body iron metabolism in CKD.

Introduction

As the incidence of chronic kidney disease (CKD) has increased worldwide, morbidity and mortality in the general population have worsened [1, 2]. Patients with

CKD often have renal anemia, and they are generally treated using both iron supplementation and an erythropoiesis-stimulating agent (ESA). However, in individuals with CKD, iron treatment may lead to over supplementation due to functional iron deficiency.

Hepcidin is a secreted protein mainly derived from the liver that plays a crucial role in the regulation of iron metabolism [3]. Specifically, hepcidin regulates iron efflux from intracellular iron by inducing the internalization and degradation of ferroportin (FPN), a cellular iron exporter [4]. Hepcidin levels are increased in patients with CKD [5], as well as in experimental animal models of CKD [6, 7]. Increased hepcidin levels in patients with CKD may impair the proper use of stored iron and lead to FPN degradation, thereby contributing to functional iron deficiency and dysregulation of iron metabolism.

Indoxyl sulfate (IS) is a protein-bound uremic toxin and a metabolite of indole, a tryptophan metabolite that is synthesized by intestinal bacteria. In healthy subjects, IS is excreted in the urine via the renal proximal tubule; however, patients with impaired renal function show reduced excretion of IS, and it accumulates in their blood [8]. The accumulation of IS further predicts renal dysfunction in CKD [9], and high serum IS levels are associated with cardiovascular diseases and mortality in CKD patients [10]. IS also induces reactive oxygen species (ROS) as well as inflammation, and exerts adverse effects on various organs [11]. AST-120, a sorbent of uremic toxin, has been shown to ameliorate CKD-related complications [12-19].

Regarding renal anemia in CKD, IS accumulation inhibits the hypoxia-inducible factor and thus reduces EPO production [20]. Furthermore, IS removal improves the effect of ESA on anemia in late-stage CKD patients [21], indicating that IS mediates renal anemia via EPO regulation. However, it is not completely clear how IS accumulation impacts iron metabolism in CKD.

In the present study, we evaluated the effect of IS on iron metabolism, and found that IS augments hepatic hepcidin production, and in a mouse model of adenine-induced CKD, mice with a high IS concentration showed increased hepatic and plasma hepcidin levels, decreased ferroportin expression in the duodenum, and increased iron content in the spleen. These changes were ameliorated by AST-120 treatment. Our findings suggest that IS accumulation leads to increases in hepcidin, which in turn dysregulates iron metabolism in CKD.

Materials and Methods

Chemicals and reagents

Indoxyl sulfate potassium salt, adenine sulfate, and AST-120 (Kremezin™) were purchased from Sigma-Aldrich (St. Louis, MO, USA), Wako Pure Chemical Industries, Ltd. (Osaka, Japan), and Kureha Corporation (Tokyo, Japan), respectively. N-acetyl cysteine (NAC), an antioxidant drug, and CH-223191, an inhibitor of AhR, were obtained from Sigma-Aldrich. The following commercially available antibodies were used for this study: anti-NRAMP2 (DMT1) antibody, anti-ferritin heavy chain

(FTH), anti-ferritin light chain (FTL), and anti-AhR antibody (Santa Cruz Biotechnology, Santa Cruz, CA, USA); anti-transferrin receptor 1 (TfR1) antibody (Zymed Technologies; Carlsbad, CA, USA); anti-FPN antibody (Alpha Diagnostics; San Antonio, TX, USA); anti-α-tubulin (San Diego, CA, USA), which was used as a protein loading control; and anti-Histone H3 antibody (Abcam, Cambridge, UK), which was used as a loading control in the case of nuclear proteins.

Experimental animals and treatment

All experimental procedures involving animals were performed in accordance with the guidelines of the Animal Research Committee of Tokushima University Graduate School (Permit Number: 13095). Eight-week-old male C57BL6/J mice were purchased from Nippon CLEA (Tokyo, Japan). The mice were maintained under conventional conditions, with a regular 12-hour light/dark cycle and free access to food (Type NMF; Oriental Yeast, Tokyo, Japan) and water during the study. Dietary adenine administration has been used to induce CKD in rodents [22]. [Animal experiment 1]: We used a new protocol involving intraperitoneal adenine administration, as previously described [23]; however, we modified the protocol of the previous study in that we administered 100 mg/kg of adenine three times per week for four weeks. One week after the start of adenine administration, serum creatinine was elevated by approximately twofold (vehicle vs. adenine: 0.50 ± 0.07 mg/dL vs. 0.87 ± 0.15 mg/dL; $p < 0.01$); the mice that were receiving adenine were then divided into two

groups and treated for three more weeks; specifically, a “normal diet” group and an “AST-120” group, in which the normal diet was supplemented with 5% AST-120, were established [13, 19]. A control group received a normal diet, as well as intraperitoneal vehicle administration. [Animal experiment 2]: To test the direct IS effect on hepcidin, 0.1% IS (200 mg (800 μmol)/kg/day) was administered to the mice in their drinking water for two weeks as previously described [19]. The mice were euthanized by intraperitoneal over-dose injection of pentobarbital, their blood was collected, and their tissue was removed and stored at -80°C until use.

Hematological analysis

Whole blood cell counts were performed by Shikoku Chuken Co. Ltd. (Kagawa, Japan), and serum creatinine levels were determined using an alkaline picrate based assay (LabAssay Creatinine Kit, Wako Pure Chemical Industries Ltd., Osaka, Japan).

Measurement of plasma iron levels, plasma ferritin levels, and tissue iron concentration

Plasma iron levels and tissue iron concentrations were measured using an iron assay kit according to the manufacturer’s instructions (Metallo Assay; Metallogenics Co. Ltd.; Chiba, Japan), as previously described [24-26]. Plasma ferritin

levels were determined by a Mouse Ferritin ELISA Kit (Immunology Consultants Laboratory, Newberg, OR) according to the manufacturer's instructions.

Cell culture

HepG2, a human hepatoma cell line, was purchased from the Japanese Collection of Research Bioresources (Osaka, Japan). The methods of cell culture have been previously described [26]. In some experiments, the cells were pre-treated for one hour with either 100 μM tempol (ROS scavenger), 10 μM BAY11-7082 (NF-κB inhibitor), 100 μM NAC (antioxidant drug), or 10 μM CH-223191 (AhR inhibitor) before stimulation with IS. In other experiments, HepG2 cells were cultured in bovine serum albumin (BSA) (40g/L) containing DMEM [11]. BSA was purchased from Wako Pure Chemical Industries, Ltd., and the concentration of endotoxin in BSA solution was 0.03 ng/mL as detected using a Limulus Amebocyte Lysate assay (Pierce™ LAL Chromogenic Endotoxin Quantitation Kit, Thermo Fisher Scientific Inc. Waltham, MA, USA).

RNA extraction and evaluation of mRNA expression levels

The RNA extraction, cDNA synthesis, and quantitative RT-PCR methods have been described previously [25]. The primer sets used were as follows: 5′ -ATGTCGCCTCCAGATACCAC-3′ and 5′ -CCTCTCCCGTGTACAGCTTC-3′ for mouse *erythropoietin* (*EPO*), 5′ -CTGCCTGTCTCCTGCTTCTC-3′ and 5′ -

AGATGCAGATGGGGAAGTTG-3′ for mouse *hepcidin-1*, 5′-CTCCGAACAATCACTGCTGA-3′ and 5′-CCTCCCCTGTGTSCSGCTTC-3′ for human *hepcidin*, 5′-CTGCCTTTCCCACAAGATGT-3′ and 5′-CAGTTATCCTGGCCTCCGTTT-3′ for human *AhR*, and 5′-GCTCCAAGCAGATGCAGCA-3′ and 5′-CCGGATGTGAGGCAGCAG-3′ for *36B4* as an internal control. The expression levels of all target genes were normalized using *36B4*, and the values were compared to the control group in terms of relative fold changes.

Protein extraction and western blot analysis

Protein preparation was done and western blotting was performed as previously described [25]. Densitometry of the visualized bands was quantified using Image J 1.38x software. Protein staining by Ponceau S solution was used as a protein loading control in the duodenum.

Measurement of intracellular reactive oxidative species levels

Intracellular ROS were detected using dichlorofluorescin diacetate (DCFH-DA; Sigma-Aldrich). HepG2 cells were stimulated, for various time periods, using 250 µM IS; then, they were incubated with 10 µM DCFH-DA at 37°C for 30 minutes. After washing, ROS production was quantified at 488 and 532 nm using a

microplate reader (FilterMax F3 Multi-Mode Microplate Reader; Molecular Devices LLC, Sunnyvale, CA, USA).

Small interfering RNA experiments

Small interfering RNA (siRNA) targeting human AhR and a non-targeting siRNA control sequence were commercially obtained from Sigma Aldrich (Mission siRNA; Tokyo, Japan). Transfection was performed as previously described [26]. Briefly, subconfluent HepG2 cells were transfected for 24 hours with 25 nM siRNA using the RNAiMAX® reagent and OPTI-MEM® (Life Technologies, Inc.). In all experiments, transfected HepG2 cells were used 48 hours after transfection.

Measurement of IS and hepcidin concentrations in plasma and cell culture medium

IS levels in mouse plasma were measured using high performance liquid chromatography. The concentrations of human and mouse hepcidin-25 were quantitatively analyzed as previously described [27]. In brief, surface-enhanced laser desorption ionization time of flight mass spectrometry (SELDI-TOF MS) was used to analyze hepcidin-25. The molecular sizes of peptides at 2789 m/z matched with the reported sizes of hepcidin-25, and the serum peptide at 2789 m/z was identified as

hepcidin-25 by collision-induced dissociation tandem MS. The assays were performed by Medical Care Proteomics Biotechnology Co. Ltd. (Kanazawa, Japan).

Evaluation of iron-regulatory protein iron-responsive element binding activity

The interaction between iron-regulatory protein (IRP) and iron-responsive element (IRE) was evaluated using an EMSA kit (LightShift Chemiluminescent RNA EMSA Kit; Thermo Fisher Scientific Inc., Rockford, IL, USA) as previously reported [24]. Semi-quantification for IRP-IRE binding activity was performed using ImageJ 1.38X software.

Statistical analysis

Data are presented as means ± standard deviation (SD). An unpaired, 2-tailed, Student's *t*-test was used for comparisons between the two groups. For comparisons between more than two groups, the statistical significance of each difference was evaluated using a post-hoc test (either Dunnett's method or Tukey-Kramer's method). *P*-values < 0.05 indicated statistical significance.

Results

Effect of IS on hepcidin expression in liver and cultured hepatic cell line

IS stimulated hepcidin mRNA expression in a dose-dependent manner in HepG2 cells (Figure 1A). Similarly, hepcidin secreted from HepG2 cells was increased by IS stimulation (Figure 1B). AhR is a receptor for IS, and activated AhR is translocated from the cytosol to the nucleus, where it promotes the transcription of target genes [28]. Indeed, IS stimulation promoted nuclear translocation of AhR in HepG2 cells at 30 minutes or later in the present study (Figure 1C). Therefore, we used RNA interference to check whether AhR is involved in IS-induced hepcidin upregulation and observed that the siRNA reduced AhR mRNA levels to 27.0 ± 3.0% of the control ($p < 0.01$) and reduced AhR protein levels to 38.9 ± 16.7% of the control ($p < 0.01$). Silencing of AhR diminished IS-induced hepcidin expression (Figure 1D). Similarly, pharmacological AhR inhibition using CH-223191 suppressed IS-induced hepcidin expression (Figure 1E). These findings suggest that IS increases hepcidin expression via an AhR-mediated pathway.

Influence of albumin on IS-induced hepcidin expression

Uremic toxins such as IS exist as protein-bound toxins in the blood. Therefore, we tested IS action on hepcidin in HepG2 cells cultured with BSA containing DMEM, and confirmed that IS augmented hepcidin mRNA expression similarly in HepG2 cells cultured with DMEM with BSA as in those cultured with

DMEM without BSA (Figure 1F). Moreover, there was no difference in basal hepcidin expression regardless of BSA inclusion.

Involvement of oxidative stress in IS-induced hepcidin expression

IS causes oxidative stress and the consequent activation of the NF-κB pathway in endothelial cells and proximal tubular cells [29-31]. Similar to previous findings, IS caused oxidative stress in HepG2 cells in the present study (Figure 2A), and the IS-induced oxidative stress was suppressed by tempol, a superoxide scavenger (Figure 2B). IS-induced hepcidin upregulation was also suppressed by NAC or BAY11-7082, an inhibitor of NF-κB (Figures 2C, D, and E). With regard to the relationship between oxidative stress and the AhR pathway, tempol failed to block IS-induced translocation of AhR to the nucleus from the cytosol (Figure 2F). Conversely, AhR knockdown did not prevent IS-mediated oxidative stress in HepG2 cells (Figure 2G). Moreover, concomitant treatment with AhR siRNA and BAY-11-7082 almost blocked IS-induced hepcidin expression (Figure 2H). These results suggest that IS-induced hepcidin expression is also mediated via the oxidative stress-NF-κB pathway, and that it is independent of the AhR pathway.

Changes in hepcidin levels in adenine-induced CKD mice

To assess iron metabolism in CKD, we used mice with adenine-induced CKD. In adenine-induced CKD mice, hepatic hepcidin expression and plasma hepcidin concentration were significantly increased four weeks after the start of adenine administration (Figure 3A and B). These increases in both hepatic hepcidin expression and plasma hepcidin concentration were diminished by AST-120 treatment. As shown in Figure 3C, hepcidin concentration was positively correlated with IS levels, suggesting that IS is closely associated with hepcidin levels. These results indicate that IS accumulation involves hepcidin regulation in CKD mice.

Alterations in tissue iron content in adenine-induced CKD mice

We examined the impact of IS accumulation on the tissue iron content in adenine-induced CKD mice. As shown in Table 2, iron content was elevated in the spleen and skeletal muscle in adenine-induced CKD mice, and these increases in iron content were subsequently restored by AST-120 treatment. Duodenal iron content was also increased in adenine-induced CKD mice, but it was not changed by AST-120 treatment. On the other hand, while CKD mice presented with decreased iron content in the liver and kidney, AST-120 did not ameliorate this effect. The findings of decreased plasma iron levels and increased plasma ferritin levels in the adenine-induced CKD mice are compatible with functional iron deficiency, and both in the iron and

ferritin levels in the blood were ameliorated by AST-120 treatment. These results indicate impaired iron distribution and utilization in CKD mice.

Ferroportin expression in the duodenum and spleen

As described above, hepcidin regulates cellular iron efflux via the internalization and degradation of FPN; hepcidin upregulation in CKD mice might therefore reduce the expression of FPN. As expected, FPN expression was diminished in the duodenum of CKD mice (Figure 4A), and its expression levels were restored by AST-120 treatment. In contrast, splenic FPN expression was augmented in CKD mice, and this change was also reversed by AST-120 (Figure 5A). In the spleens of CKD mice, FPN mRNA expression was increased and IRP-IRE binding activity was reduced, which was consistent with the increased FPN protein expression. The changes in FPN mRNA and IRP activity were also improved by AST-120 treatment, which corresponded with the reduction of FPN expression (Figure 5G and H). IRP-IRE binding activity was regulated by iron content, and the change in IRP activity corresponded with changes in splenic iron content. These findings suggest that FPN is post-transcriptionally regulated, independently of hepcidin, in the spleens of CKD mice.

The protein expression of iron importers and iron storage in the duodenum and spleen

Next, we examined the protein expression of iron importers and iron storage in the duodenum and spleen. In the duodenum, the expression levels of DMT1, FTH, and FTL did not differ among the three groups (Figure 4B-D). Although no difference in DMT1 expression was seen, levels of TfR were decreased, and those of FTH and FTL were elevated in the spleens of CKD mice. These changes were all reversed by AST-120 treatment (Figure 5B-E). Moreover, splenic hepcidin expression was significantly reduced in adenine-induced CKD mice, which tended to be restored by AST-120 treatment (Figure 5F).

Effect of IS removal on anemia in adenine-induced CKD mice

Adenine-induced CKD mice demonstrated microcytic hypochromic anemia after four weeks of adenine treatment (Table 3). Treatment using AST-120 improved impaired iron absorption and utilization in adenine-induced CKD mice, and renal anemia was partly prevented by AST-120 treatment. CKD-induced elevation of plasma creatinine was slightly suppressed by AST-120 at four weeks (Table 1), and renal EPO expression remained at low levels in CKD mice, despite AST-120 treatment (Figure 6). In addition, there were no differences in plasma creatinine and the degree of anemia between the adenine-CKD mice and the adenine-CKD mice treated with AST-120 after two weeks of adenine treatment and one week of AST-120 treatment (Tables 1 and 3). These data

suggest that AST-120 restored iron incorporation and utilization by suppressing a pathway that is hepcidin/FPN-dependent and EPO-independent.

Changes in mRNA expression of the inflammatory cytokines

IL-6 plays an important role in hepcidin regulation [32]. We examined the participation of inflammatory cytokines in hepcidin expression in adenine-CKD mice. As shown in Figure 7, the mRNA expression of IL-6, as well as IL-1ß and TNF-α, was increased in the kidneys of adenine-CKD mice. In contrast, the mRNA expression of those genes was decreased in the livers of adenine-CKD mice, indicating a lack of involvement of inflammatory cytokines in hepcidin regulation in the livers of adenine-CKD mice.

Direct effect of IS on hepcidin in mice with IS treatment

We examined whether IS has a direct effect on hepatic hepcidin expression using mice that had been administered IS. IS treatment augmented hepatic hepcidin mRNA expression as well as plasma hepcidin concentration (Figure 8A and B). IS administration also induced mild anemia despite no difference in plasma creatinine levels between the control mice and those that were administered IS (Figure 8C and

Table 4). Therefore, IS directly affects hepcidin regulation independent of renal function.

Discussion

In the *in vitro* experiments of the present study, IS augmented hepatic hepcidin expression via a pathway that depended on both AhR and oxidative stress. Similarly, hepatic and plasma hepcidin levels were increased in the *in vivo* experiments using adenine-induced CKD mice. The CKD mice also showed decreased FPN expression in the duodenum and increased splenic iron concentrations. The alterations in iron metabolism in the CKD mice were ameliorated by AST-120, which removes IS. These observations suggest, for the first time, the involvement of IS in iron metabolism in CKD.

Hepcidin was first identified as an antimicrobial peptide and it plays an important role in the regulation of iron metabolism [3]. Specifically, hepcidin regulates cellular iron efflux via both the internalization and degradation of FPN [4]. Therefore, CKD-related increases in hepcidin levels contribute to the intracellular sequestration of iron, as well as impaired absorption of iron from the duodenum, and such changes promote functional iron deficiency in CKD. Indeed, several studies have shown that

the serum hepcidin concentration is elevated in CKD, which contributes to whole-body iron dysregulation. Moreover, elevated serum hepcidin levels are correlated with serum ferritin levels and inflammatory markers in patients with CKD [5]. Adenine-induced CKD animals show increases in hepatic hepcidin, as well as abnormal iron metabolism [6, 7]. In the present study, we found that hepatic hepcidin expression and plasma hepcidin concentration were elevated in adenine-induced CKD mice. These hepcidin increases were rectified by the removal of IS. The present study is the first to reveal the association between IS and hepcidin regulation.

To investigate the mechanism by which IS regulates hepcidin concentrations, we used HepG2 cells and found that IS also increased hepcidin expression in these cells. Previously, Schroeder et al. demonstrated that IS is a ligand of AhR, and that IS acts via AhR [28]. In the current investigation, IS promoted the translocation of AhR to the nucleus from the cytosol in HepG2 cells, and the IS-induced hepcidin upregulation was reversed by AhR silencing. Similarly, previous studies have shown that various IS actions are prevented by AhR silencing [33]. Taken together, clearly the effect of IS on hepcidin is exerted through an AhR-mediated pathway.

IS is known to cause oxidative stress; consequently, the toxin activates NF-κB signaling [29-31, 34]. In the present study, IS-induced hepcidin augmentation was suppressed by both a free radical scavenger and an NF-κB inhibitor, suggesting that the IS-induced oxidative stress-NF-κB axis is involved in hepcidin regulation.

However, IS-induced oxidative stress was not reduced by AhR siRNA, and tempol did not inhibit the IS-induced translocation of AhR to the nucleus. In addition, IS-induced hepcidin upregulation was almost completely abolished by the simultaneous inhibition of the AhR and NF-κB pathways. These results suggest that IS/oxidative stress-induced hepcidin expression occurs independently of any AhR-mediated pathway.

In contrast to our results, several studies have shown that hepcidin is downregulated by oxidative stress induced by alcohol [35] or the hepatitis C virus [36]. However, pathophysiologically relevant H_2O_2 levels have been shown to upregulate hepcidin expression via STAT3 [37]. In terms of the effect of NF-κB on hepcidin, a previous study showed that LPS-induced hepcidin upregulation is mediated by NF-κB–dependency, which is similar to our finding [38]. In contrast, ceramide-induced hepcidin regulation is not involved in the NF-κB pathway [39]. Therefore, oxidative stress and NF-κB have dual characteristics as either positive or negative regulators of hepcidin.

Uremic solutes normally exist as protein-bound toxins, and several studies, including the present study, used high concentrations of IS relative to the concentrations in uremic CKD patients in the *in vitro* experiments [11, 40]. Therefore, we tested the IS effect on hepcidin in HepG2 cells by using both the free concentration (25μM) in albumin-free DMEM and the protein-bound maximum concentration (250 μM) in DMEM containing BSA. Twenty-five μM of IS induced an approximately

twofold increase in hepcidin mRNA expression in HepG2 cultured with BSA-free DMEM, and 250 μM IS also increased hepcidin mRNA expression in HepG2 cultured with BSA-containing DMEM. In addition, there was no difference in basal hepcidin mRNA expression in DMEM regardless of BSA inclusion, indicating no impact of albumin on hepcidin expression (Figure 1F). Thus, hepcidin expression was upregulated by IS at the free concentration and protein-bound concentration doses in HepG2 cells under our experimental condition.

Inflammatory cytokines (i.e., IL-6) are also important factors in hepcidin regulation [32]. As expected, the expression of IL-6, IL-1ß, and TNF-α mRNA was upregulated in the kidney in CKD mice. However, it was decreased in the liver. Although the reason for the discrepancy in inflammatory cytokine expression between the kidney and liver remains unclear, inflammatory cytokines might not be associated with the regulation of hepatic hepcidin in an adenine-induced CKD mouse model.

Regarding alterations in iron distribution in CKD mice, iron concentrations in the spleen, duodenum, and skeletal muscle were increased. Plasma ferritin was also increased, though plasma iron was decreased, indicating that iron absorption and utilization were impaired. These alterations were mostly ameliorated by AST-120 treatment. It follows that IS removal, and the resulting inhibition of hepcidin, might improve (1) iron metabolism and (2) iron utilization in CKD. Consistent with this result, decreased expression of FPN in the duodenum was restored by AST-120

treatment in CKD mice, indicating that IS removal affects hepcidin levels. Conversely, CKD mice showed increased FPN expression in the spleen, which was reduced by AST-120 treatment. It is not clear why the discrepancy of increased FPN expression in the spleen combined with elevated hepcidin in the liver and serum is present in CKD mice. FPN expression is controlled by both transcriptional and post-transcriptional regulation, as well as by the translational regulation of hepcidin-dependent internalization. In macrophages, FPN transcription is induced by iron, as well as by heme protein [41]. Additionally, FPN mRNA has an iron-responsive element in the 5′ -region [42], and its translation is therefore increased by high iron levels because it can bind to iron regulatory protein 1 [43]. In the spleens of CKD mice, FPN mRNA was increased and IRP activity was reduced, which is consistent with the understanding that increased FPN protein expression is responsible for the transcriptional upregulation. Therefore, we suggest that the increased FPN expression seen in CKD mice is likely responsible for the accumulation of iron in the spleen, and that this accumulation overwhelms hepcidin-mediated mechanisms. In addition, hepcidin expression has been observed in not only the liver, but also the heart [44], kidney [45], brain [46], and spleen [47]. Although the function of extra-hepatic hepcidin remains unknown, it might influence local iron regulation. In the present study, hepcidin expression was reduced in the spleens of adenine-CKD mice, indicating the involvement of local hepcidin on the regulation of splenic FPN expression. Further examination is necessary to clarify

whether there is a coordinated regulation of (1) peripheral FPN expression or (2) hepatic hepcidin levels.

CKD mice showed renal anemia compatible with iron-deficient anemia, which is caused by iron sequestration and impaired iron utilization, as well as by reduced renal EPO production. The renal anemia was slightly improved by AST-120 treatment, perhaps because consequent reductions in hepcidin restored iron utilization. In previous studies, hepcidin inhibition ameliorated erythropoiesis in (1) a model of CKD combined with renal anemia, (2) hepcidin-deficient mice, and (3) mice that had been treated with a hepcidin inhibitor [7, 48]. This suggests that hepcidin inhibition mobilizes iron and improves iron utilization. In the same way, the removal of IS using AST-120 ameliorated iron accumulation in the spleen and skeletal muscle, as well as elevated plasma ferritin levels. Conversely, the treatment reduced plasma iron levels in CKD mice, indicating that iron mobilization in tissues with ectopic iron accumulation had been improved. Moreover, AST-120 slowed the progression of renal dysfunction, as estimated by plasma creatinine level; however, the decrease of renal EPO expression in CKD mice was not changed by IS removal. Therefore, IS removal ameliorates renal anemia via the restoration of iron utilization rather than through increased EPO production. Additionally, cyanate, formed spontaneously from accumulated urea, decreases EPO activity in order to induce EPO carbamylation [49, 50], which might promote inadequate erythropoiesis in CKD.

A recent clinical study (Evaluating Prevention of Progression in CKD [EPPIC] trials) demonstrated that AST-120 fails to prevent disease progression in patients with moderate to severe CKD [51]. Moreover, a subgroup analysis within the EPPIC study revealed that AST-120 delays the primary end point (dialysis initiation, kidney transplantation, or serum creatinine doubling) in American patients [52]. Thus, it remains controversial whether IS removal prevents renal dysfunction in CKD. Nonetheless, the uremic toxicity of IS accumulation causes dysfunction in various organs through multiple pathways. Further examination is necessary to elucidate the effect of AST-120 on renal anemia in CKD.

In conclusion, IS induces hepcidin production via a pathway that involves both AhR and oxidative stress; this results in iron sequestration and impaired iron utilization in CKD. AST-120 ameliorates iron metabolism by inhibiting hepcidin increases, promoting iron mobilization, and ameliorating erythropoiesis. These findings suggest that a therapeutic strategy of uremic toxin removal may be useful for correcting impaired iron metabolism in CKD.

Acknowledgements

We appreciate the excellent technical advice given by the Support Center for Advanced Medical Sciences, Institute of Biomedical Sciences, Tokushima University Graduate School. We would like to thank Editage (www.editage.jp) for the English language editing services.

Conflict of Interest Statement

The authors declare no competing financial interests.

Authors' Contributions

1. Study conception and design: Y.I.

2. Experimentation and data acquisition: H.H., Y.I., and H.W.

3. Analysis and interpretation of data: H.H., Y.I., H.W., Y.H., Y.I.-I, M.I., Y.Z., K.T., L.M., K.I., K.T., and T.T.

4. Writing or critically revision of the manuscript for important intellectual content: H.H., Y.I., Y.H., and T.T.

5. Final approval of the version to be published: All authors.

Funding

This work was supported by a research grant from the Kojinkai Foundation, the President discretion research budget of the University of Tokushima, and JSPS KAKENHI (Grant Number JP17H00503) to H.H. Further grants were provided to Y.I. by the Ichiro Kanehara Foundation for the Promotion of Medical Sciences and Medical Care, the pathophysiological research conference in chronic kidney disease (JKFB15-12), and partly by the JSPS KAKENHI (Grant Number JP15K01716 to Y.I., Grant Number JP15H02898 to T.T.).

Reference

1. Collins AJ, Foley RN, Gilbertson DT, *et al.* The state of chronic kidney disease, ESRD, and morbidity and mortality in the first year of dialysis. Clin J Am Soc Nephrol 2009;4 Suppl 1:S5-11
2. Go AS, Chertow GM, Fan D, *et al.* Chronic kidney disease and the risks of death, cardiovascular events, and hospitalization. N Engl J Med 2004;351(13):1296-1305
3. Park CH, Valore EV, Waring AJ, *et al.* Hepcidin, a urinary antimicrobial peptide synthesized in the liver. J Biol Chem 2001;276(11):7806-7810
4. Nemeth E, Tuttle MS, Powelson J, *et al.* Hepcidin regulates cellular iron efflux by binding to ferroportin and inducing its internalization. Science 2004;306(5704):2090-2093
5. Zaritsky J, Young B, Wang HJ, *et al.* Hepcidin--a potential novel biomarker for iron status in chronic kidney disease. Clin J Am Soc Nephrol 2009;4(6):1051-1056
6. Hamada Y, Kono TN, Moriguchi Y, *et al.* Alteration of mRNA expression of molecules related to iron metabolism in adenine-induced renal failure rats: a possible mechanism of iron deficiency in chronic kidney disease patients on treatment. Nephrol Dial Transplant 2008;23(6):1886-1891
7. Sun CC, Vaja V, Chen S, *et al.* A hepcidin lowering agent mobilizes iron for incorporation into red blood cells in an adenine-induced kidney disease model of anemia in rats. Nephrol Dial Transplant 2013;28(7):1733-1743
8. Niwa T, Takeda N, Tatematsu A, *et al.* Accumulation of indoxyl sulfate, an inhibitor of drug-binding, in uremic serum as demonstrated by internal-surface reversed-phase liquid chromatography. Clin Chem 1988;34(11):2264-2267
9. Wu IW, Hsu KH, Lee CC, *et al.* p-Cresyl sulphate and indoxyl sulphate predict progression of chronic kidney disease. Nephrol Dial Transplant 2011;26(3):938-947
10. Barreto FC, Barreto DV, Liabeuf S, *et al.* Serum indoxyl sulfate is associated with vascular disease and mortality in chronic kidney disease patients. Clin J Am Soc Nephrol 2009;4(10):1551-1558
11. Vanholder R, Schepers E, Pletinck A, *et al.* The uremic toxicity of indoxyl sulfate and p-cresyl sulfate: a systematic review. J Am Soc Nephrol 2014;25(9):1897-1907
12. Nishikawa M, Ishimori N, Takada S, *et al.* AST-120 ameliorates lowered exercise capacity and mitochondrial biogenesis in the skeletal muscle from mice with chronic kidney disease via reducing oxidative stress. Nephrol Dial Transplant 2015;30(6):934-942
13. Yamamoto S, Zuo Y, Ma J, *et al.* Oral activated charcoal adsorbent (AST-120) ameliorates extent and instability of atherosclerosis accelerated by kidney disease in apolipoprotein E-deficient mice. Nephrol Dial Transplant 2011;26(8):2491-2497

14. Six I, Gross P, Remond MC, *et al.* Deleterious vascular effects of indoxyl sulfate and reversal by oral adsorbent AST-120. Atherosclerosis 2015;243(1):248-256
15. Inami Y, Hamada C, Seto T, *et al.* Effect of AST-120 on Endothelial Dysfunction in Adenine-Induced Uremic Rats. Int J Nephrol 2014;2014:164125
16. Yu M, Kim YJ, Kang DH. Indoxyl sulfate-induced endothelial dysfunction in patients with chronic kidney disease via an induction of oxidative stress. Clin J Am Soc Nephrol 2011;6(1):30-39
17. Iwasaki Y, Kazama JJ, Yamato H, *et al.* Accumulated uremic toxins attenuate bone mechanical properties in rats with chronic kidney disease. Bone 2013;57(2):477-483
18. Komiya T, Miura K, Tsukamoto J, *et al.* Possible involvement of nuclear factor-kappaB inhibition in the renal protective effect of oral adsorbent AST-120 in a rat model of chronic renal failure. Int J Mol Med 2004;13(1):133-138
19. Ito S, Higuchi Y, Yagi Y, *et al.* Reduction of indoxyl sulfate by AST-120 attenuates monocyte inflammation related to chronic kidney disease. J Leukoc Biol 2013;93(6):837-845
20. Chiang CK, Tanaka T, Inagi R, *et al.* Indoxyl sulfate, a representative uremic toxin, suppresses erythropoietin production in a HIF-dependent manner. Lab Invest 2011;91(11):1564-1571
21. Wu IW, Hsu KH, Sun CY, *et al.* Oral adsorbent AST-120 potentiates the effect of erythropoietin-stimulating agents on Stage 5 chronic kidney disease patients: a randomized crossover study. Nephrol Dial Transplant 2014;29(9):1719-1727
22. Tanaka T, Doi K, Maeda-Mamiya R, *et al.* Urinary L-type fatty acid-binding protein can reflect renal tubulointerstitial injury. Am J Pathol 2009;174(4):1203-1211
23. Al Za'abi M, Al Busaidi M, Yasin J, *et al.* Development of a new model for the induction of chronic kidney disease via intraperitoneal adenine administration, and the effect of treatment with gum acacia thereon. Am J Transl Res 2015;7(1):28-38
24. Tajima S, Ikeda Y, Enomoto H, *et al.* Angiotensin II alters the expression of duodenal iron transporters, hepatic hepcidin, and body iron distribution in mice. Eur J Nutr 2015;54(5):709-719
25. Ikeda Y, Imao M, Satoh A, *et al.* Iron-induced skeletal muscle atrophy involves an Akt-forkhead box O3-E3 ubiquitin ligase-dependent pathway. J Trace Elem Med Biol 2016;35:66-76
26. Ikeda Y, Tajima S, Izawa-Ishizawa Y, *et al.* Estrogen regulates hepcidin expression via GPR30-BMP6-dependent signaling in hepatocytes. PLoS One 2012;7(7):e40465
27. Tomosugi N, Kawabata H, Wakatabe R, *et al.* Detection of serum hepcidin in renal failure and inflammation by using ProteinChip System. Blood 2006;108(4):1381-1387
28. Schroeder JC, Dinatale BC, Murray IA, *et al.* The uremic toxin 3-indoxyl sulfate is a potent endogenous agonist for the human aryl hydrocarbon receptor. Biochemistry 2010;49(2):393-400

29. Masai N, Tatebe J, Yoshino G, *et al.* Indoxyl sulfate stimulates monocyte chemoattractant protein-1 expression in human umbilical vein endothelial cells by inducing oxidative stress through activation of the NADPH oxidase-nuclear factor-kappaB pathway. Circ J 2010;74(10):2216-2224
30. Shimizu H, Yisireyili M, Higashiyama Y, *et al.* Indoxyl sulfate upregulates renal expression of ICAM-1 via production of ROS and activation of NF-kappaB and p53 in proximal tubular cells. Life Sci 2013;92(2):143-148
31. Tumur Z, Shimizu H, Enomoto A, *et al.* Indoxyl sulfate upregulates expression of ICAM-1 and MCP-1 by oxidative stress-induced NF-kappaB activation. Am J Nephrol 2010;31(5):435-441
32. Nemeth E, Rivera S, Gabayan V, *et al.* IL-6 mediates hypoferremia of inflammation by inducing the synthesis of the iron regulatory hormone hepcidin. J Clin Invest 2004;113(9):1271-1276
33. Asai H, Hirata J, Hirano A, *et al.* Activation of aryl hydrocarbon receptor mediates suppression of hypoxia-inducible factor-dependent erythropoietin expression by indoxyl sulfate. Am J Physiol Cell Physiol 2016;310(2):C142-150
34. Shimizu H, Bolati D, Adijiang A, *et al.* NF-kappaB plays an important role in indoxyl sulfate-induced cellular senescence, fibrotic gene expression, and inhibition of proliferation in proximal tubular cells. Am J Physiol Cell Physiol 2011;301(5):C1201-1212
35. Harrison-Findik DD, Schafer D, Klein E, *et al.* Alcohol metabolism-mediated oxidative stress down-regulates hepcidin transcription and leads to increased duodenal iron transporter expression. J Biol Chem 2006;281(32):22974-22982
36. Miura K, Taura K, Kodama Y, *et al.* Hepatitis C virus-induced oxidative stress suppresses hepcidin expression through increased histone deacetylase activity. Hepatology 2008;48(5):1420-1429
37. Millonig G, Ganzleben I, Peccerella T, *et al.* Sustained submicromolar H2O2 levels induce hepcidin via signal transducer and activator of transcription 3 (STAT3). J Biol Chem 2012;287(44):37472-37482
38. Wu S, Zhang K, Lv C, *et al.* Nuclear factor-kappaB mediated lipopolysaccharide-induced mRNA expression of hepcidin in human peripheral blood leukocytes. Innate Immun 2012;18(2):318-324
39. Lu S, Natarajan SK, Mott JL, *et al.* Ceramide Induces Human Hepcidin Gene Transcription through JAK/STAT3 Pathway. PLoS One 2016;11(1):e0147474
40. Duranton F, Cohen G, De Smet R, *et al.* Normal and pathologic concentrations of uremic toxins. J Am Soc Nephrol 2012;23(7):1258-1270
41. Marro S, Chiabrando D, Messana E, *et al.* Heme controls ferroportin1 (FPN1) transcription involving Bach1, Nrf2 and a MARE/ARE sequence motif at position -7007 of the FPN1 promoter. Haematologica 2010;95(8):1261-1268
42. Abboud S, Haile DJ. A novel mammalian iron-regulated protein involved in intracellular iron metabolism. J Biol Chem 2000;275(26):19906-19912

43. Rouault TA. The role of iron regulatory proteins in mammalian iron homeostasis and disease. Nat Chem Biol 2006;2(8):406-414
44. Merle U, Fein E, Gehrke SG, *et al.* The iron regulatory peptide hepcidin is expressed in the heart and regulated by hypoxia and inflammation. Endocrinology 2007;148(6):2663-2668
45. Kulaksiz H, Theilig F, Bachmann S, *et al.* The iron-regulatory peptide hormone hepcidin: expression and cellular localization in the mammalian kidney. J Endocrinol 2005;184(2):361-370
46. McCarthy RC, Kosman DJ. Glial cell ceruloplasmin and hepcidin differentially regulate iron efflux from brain microvascular endothelial cells. PLoS One 2014;9(2):e89003
47. Peyssonnaux C, Zinkernagel AS, Datta V, *et al.* TLR4-dependent hepcidin expression by myeloid cells in response to bacterial pathogens. Blood 2006;107(9):3727-3732
48. Akchurin O, Sureshbabu A, Doty SB, *et al.* Lack of hepcidin ameliorates anemia and improves growth in an adenine-induced mouse model of chronic kidney disease. Am J Physiol Renal Physiol 2016;311(5):F877-F889
49. Mun KC, Golper TA. Impaired biological activity of erythropoietin by cyanate carbamylation. Blood Purif 2000;18(1):13-17
50. Park KD, Mun KC, Chang EJ, *et al.* Inhibition of erythropoietin activity by cyanate. Scand J Urol Nephrol 2004;38(1):69-72
51. Schulman G, Berl T, Beck GJ, *et al.* Randomized Placebo-Controlled EPPIC Trials of AST-120 in CKD. J Am Soc Nephrol 2015;26(7):1732-1746
52. Schulman G, Berl T, Beck GJ, *et al.* The effects of AST-120 on chronic kidney disease progression in the United States of America: a post hoc subgroup analysis of randomized controlled trials. BMC Nephrol 2016;17(1):141

Table 1. Characteristics of the control mice and adenine-CKD mice with or without AST-120 treatment

	1W		2W			4W		
	Control	Adenine	Control	Adenine	Adenine+AST120	Control	Adenine	Adenine +AST120
Body weight (g)	24.7 ± 2.2	22.5 ± 0.7	26.8 ± 1.1	20.8 ± 1.8**	20.4 ± 0.6**	28.2 ± 2.0	18.2 ± 1.5**	18.5 ± 1.3**
Right kidney weight (mg)	131.5 ± 12.5	163.8 ± 14.4*	143.0 ± 10.4	179.3 ± 17.6*	148.5 ± 14.1#	156.9 ± 10.5	152.1 ± 13.3	158.9 ± 12.2
Left kidney weight (mg)	122.3 ± 13.2	156.3 ± 14.2**	143.8 ± 13.4	170.3 ± 7.5	149 ± 15.2	149.7 ± 10.9	148.7 ± 17.5	153.9 ± 17.5
Plasma creatinine (mg/dL)	0.50 ± 0.07	0.87 ± 0.15**	0.31 ± 0.07	1.08 ± 0.21**	0.97 ± 0.03**	0.36 ± 0.11	1.67 ± 0.38**	1.33 ± 0.33**#

Data are presented as means ± SD; n = 4-15, respectively. *P < 0.05, **P < 0.01 vs. control mice at the same week. #P < 0.05, ##P < 0.01 vs. adenine diet at the same week.

IS; indoxyl sulfate.

Table 2. Tissue iron content, plasma iron levels, and plasma ferritin concentration

	Control	Adenine	Adenine + AST-120
Spleen (μg/g tissue weight)	6.1 ± 1.1	19.0 ± 7.5*	8.4 ± 0.9#
Liver (μg/g tissue weight)	19.9 ± 3.8	9.3 ± 1.3**	9.8 ± 1.3**
Duodenum (μg/g tissue weight)	8.0 ± 3.9	14.3 ± 6.9*	11.5 ± 5.7
Kidney (μg/g tissue weight)	7.6 ± 3.7	1.4 ± 0.7**	2.4 ± 1.5*
Gastrocnemius muscle (μg/g tissue weight)	3.6 ± 2.7	7.7 ± 5.4**	3.1 ± 0.6#
Plasma iron (μg/dL)	108.5 ± 16.8	78.6 ± 22.9*	111.7 ± 36.6#
Plasma ferritin (ng/mL)	504 ± 146	2842 ± 726**	1882 ± 571**##

Data are presented as means ± SD; n = 3-14, respectively. *P < 0.05, **P < 0.01 vs. control mice. #P < 0.05, ##P < 0.01 vs. adenine diet.

Table 3. Hematological data of the control mice and adenine-CKD mice with or without AST-120 treatment

	1W		2W			4W		
	Control	Adenine	Control	Adenine	Adenine+AST120	Control	Adenine	Adenine+AST120
RBC (× 10^4/μL)	914 ± 79	726 ± 68*	857 ± 26	688 ± 93*	720 ± 40*	901 ± 63	643 ± 57**	718 ± 99**#
Hb (g/dL)	14.2 ± 1.2	11.4 ± 1.0*	13.7 ± 0.3	10.1 ± 1.4**	10.6 ± 0.7*	13.7 ± 0.9	8.8 ± 0.7**	10.1 ± 1.5**#
Ht (%)	43.4 ± 3.5	32.4 ± 3.1*	39.6 ± 0.9	29.7 ± 4.5**	31.4 ± 1.7**	40.7 ± 3.1	26.8 ± 2.5**	31.4 ± 7.0**#
MCV (fL)	47.7 ± 0.6	44.5 ± 0.5**	46.3 ± 0.5	43.0 ± 1.3**	43.7 ± 0.5**	45.3 ± 0.8	41.7 ± 1.0**	43.4 ± 3.3
MCH (pg)	15.5 ± 0.1	15.7 ± 0.6	15.9 ± 0.2	14.7 ± 0.2**	14.8 ± 0.2**	15.2 ± 0.4	14.0 ± 0.3**	14.0 ± 0.3**
MCHC (g/dL)	32.7 ± 0.4	35.2 ± 1.2**	34.5 ± 0.1	34.2 ± 1.0	33.9 ± 0.4	33.8 ± 1.3	33.5 ± 1.1	32.5 ± 2.3
WBC (/μL)	5200 ± 2100	3700 ± 700	3700 ± 1300	4300 ± 1800	4600 ± 2600	5200 ± 3200	2600 ± 1100**	2900 ± 1200*
Plt (× 10^4/μL)	51.8 ± 5.2	68.0 ± 12.6*	51.0 ± 12.2	66.3 ± 17.9	63.6 ± 17.6	45.2 ± 16.2	79.3 ± 15.3**	94.6 ± 18.7**

Data are presented as means ± SD; n = 3-15, respectively. *P < 0.05, **P < 0.01 vs. control mice at the same week. #P < 0.05, ##P < 0.01 vs. adenine diet at the same week.

RBC; red blood cell, Hb; hemoglobin, Ht; hematocrit, MCV; mean corpuscular volume, MCH; mean corpuscular hemoglobin, MCHC; mean corpuscular hemoglobin concentration, WBC; white blood cell, Plt; platelet.

Table 4. Characteristics and hematological data of mice with vehicle- or IS-treatment for two weeks

	Vehicle	**IS**
Body weight (g)	27.6 ± 2.4	27.8 ± 0.3
Right kidney weight (mg)	155.3 ± 11.0	163.8 ± 22.5
Left kidney weight (mg)	152.0 ± 9.9	159.5 ± 8.9
Plasma creatinine (mg / dL)	0.37 ± 0.14	0.42 ± 0.22
RBC (× 10^4/μL)	955 ± 53	721 ± 62**
Hb (g/dL)	14.5 ± 0.9	11.3 ± 0.9**
Ht (%)	44.7 ± 2.9	33.4 ± 3.1**
MCV (fL)	46.5 ± 0.6	46.3 ± 0.5
MCH (pg)	15.2 ± 0.1	15.7 ± 0.4
MCHC (g/dL)	32.5 ± 0.5	33.9 ± 1.2
WBC (/μL)	4300 ± 900	5600 ± 1400
Plt (× 10^4/μL)	39.7 ± 7.0	50.7 ± 6.9

Data are presented as means ± SD; $n = 4$, respectively. *$P < 0.05$, **$P < 0.01$ vs. vehicle mice.

Figure legends

Figure 1. Effect of indoxyl sulfate (IS) on hepcidin expression in liver and HepG2 cells. (A) IS induces hepcidin mRNA expression in HepG2 cells in a dose-dependent manner. Values are expressed as means ± SD. *P < 0.05, **P < 0.01 (vs. vehicle treatment); n = 6-8 in each group. (B) Hepcidin concentration secreted from HepG2 cell to culture media. Values are expressed as means ± SD. *P < 0.05 (vs. vehicle treatment); n = 4 in each group. (C) IS translocates aryl hydrocarbon receptor (AhR) to the nucleus from the cytoplasm in HepG2 cells. Left panel: representative protein expression levels of AhR and tubulin, and semi-quantitative densitometry analysis of AhR expression in the cytoplasm. Right panels: representative protein expression of AhR and Histone-H3, and semi-quantitative densitometry analysis of AhR expression in the nucleus. Values are expressed as means ± SD. *P < 0.05, **P < 0.01 (vs. time at 0 min); n = 5 in each group. (D) Treatment with AhR siRNA inhibits IS-induced hepcidin upregulation in HepG2 cells. Forty-eight hours after siRNA transfection, cells were treated with either IS or vehicle. Values are expressed as means ± SD. *P < 0.05, **P < 0.01; n = 14 in each group. (E) Treatment with CH-223191 inhibits IS-induced hepcidin upregulation in HepG2 cells. Cells were treated with either IS or vehicle 1 hour after CH-223191 pretreatment. Values are expressed as means ± SD. **P < 0.01; n = 3 in each group. (F)

High concentration of IS action on hepcidin mRNA in HepG2 cells cultured with or without BSA-containing DMEM. Values are expressed as means ± SD. *P < 0.05, **P < 0.01; n = 7 in each group.

Figure 2. Effect of IS-induced oxidative stress on hepcidin expression in HepG2 cells. (A) Time course of IS-induced oxidative stress, as detected using 2′,7′-dichlorofluorescin diacetate fluorescence. IS induces oxidative stress at 15 minutes or later. Values are expressed as means ± SD. *P < 0.05, **P < 0.01 (vs. time at 0 min); n = 7–8 in each group. (B) Pre-treatment with tempol inhibits IS-induced oxidative stress in HepG2 cells. Cells were treated with either IS or vehicle for 24 hours after pre-treatment with either vehicle or tempol. Values are expressed as means ± SD. *P < 0.05, **P < 0.01; n = 8 in each group. (C) The effect of tempol, a superoxide scavenger, (D) N-acetyl cysteine, an-anti-oxidant agent, or (E) BAY-11-7082, an NF-κB inhibitor, on IS-induced oxidative stress in HepG2 cells. Values are expressed as means ± SD. *P < 0.05, **P < 0.01; n = 4-9 in each group. (F) Tempol has no inhibitory effect on IS-induced AhR translocation to the nucleus from the cytosol. Values are expressed as means ± SD. *P < 0.05, **P < 0.01; n = 8 in each group. (G) Effect of AhR silencing on IS-induced oxidative stress. Values are expressed as means ± SD. **P < 0.01; n = 11–16 in each group. (H) The concomitant effect of AhR siRNA transfection and NF-κB

inhibitor administration on IS-induced hepcidin expression in HepG2 cells. Values are expressed as means ± SD. **P < 0.01; n = 4 in each group.

Figure 3. Changes in hepcidin levels in adenine-induced CKD mice with or without AST-120 treatment. (A) Hepcidin mRNA expression. Values are expressed as means ± SD. *P < 0.05, **P < 0.01, n = 4–11 in each group. (B) Plasma hepcidin concentration. Values are expressed as means ± SD. **P < 0.01; n = 4–8 in each group. (C) Plasma indoxyl sulfate concentration. Values are expressed as means ± SD. *P < 0.05, **P < 0.01; n = 4–8 in each group. (D) Positive correlation between plasma hepcidin and IS concentration.

Figure 4. Changes in the expression of duodenal iron metabolism-related proteins in mice. Upper panel: Representative immunoblots for (A) FPN, (B) DMT1, (C) FTH, (D) FTL and protein staining. Lower panel: Semi-quantitative densitometric analyses of DMT1, FPN, FTH, and FTL protein levels normalized to protein staining. Values are expressed as means ± SD. **P < 0.01; n = 11–15 in each group.

Figure 5. Alterations in iron metabolism-related proteins in the spleen of mice. Upper panel: Representative immunoblots for (A) FPN, (B) DMT1, (C) TfR, (D) FTH, (E) FTL and tubulin. Lower panel: Semi-quantitative densitometric analyses of FPN,

DMT1, TfR, FTH, and FTL protein levels normalized to tubulin. Values are expressed as means ± SD. **P < 0.01; n = 14–18 in each group. The mRNA expression of (F) hepcidin and (G) FPN in the spleen of mice. Values are expressed as means ± SD. *P < 0.05, **P < 0.01; n = 7–12 in each group. (H) Upper panel: Representative IRP–IRE-binding bands. Lower panel: Semi-quantitative densitometry analysis of IRP activity in the spleen. *P < 0.05, **P < 0.01; n = 5 in each group.

Figure 6. Erythropoietin mRNA expression in the kidney. Values are expressed as means ± SD. **P < 0.01; n = 10–11 in each group.

Figure 7. IL-6, IL-1ß, and TNF-α mRNA expression in the kidney and liver of control mice and adenine-CKD mice. Values are expressed as means ± SD. *P < 0.05, **P < 0.01; n = 3-7 in each group.

Figure 8. (A) Hepcidin mRNA expression in the liver of vehicle-treated or IS-treated mice at 2 weeks. Values are expressed as means ± SD. ***P* < 0.01 (vs. vehicle treatment); n = 3–4 in each group. (B) Plasma hepcidin concentration. Values are expressed as means ± SD. **P* < 0.05 (vs. vehicle treatment); n = 7–11 in each group. (C) Plasma indoxyl sulfate concentration. Values are expressed as means ± SD. ***P* < 0.05 (vs. vehicle treatment); n = 4–8 in each group.

Figure 1 Hamano et al.

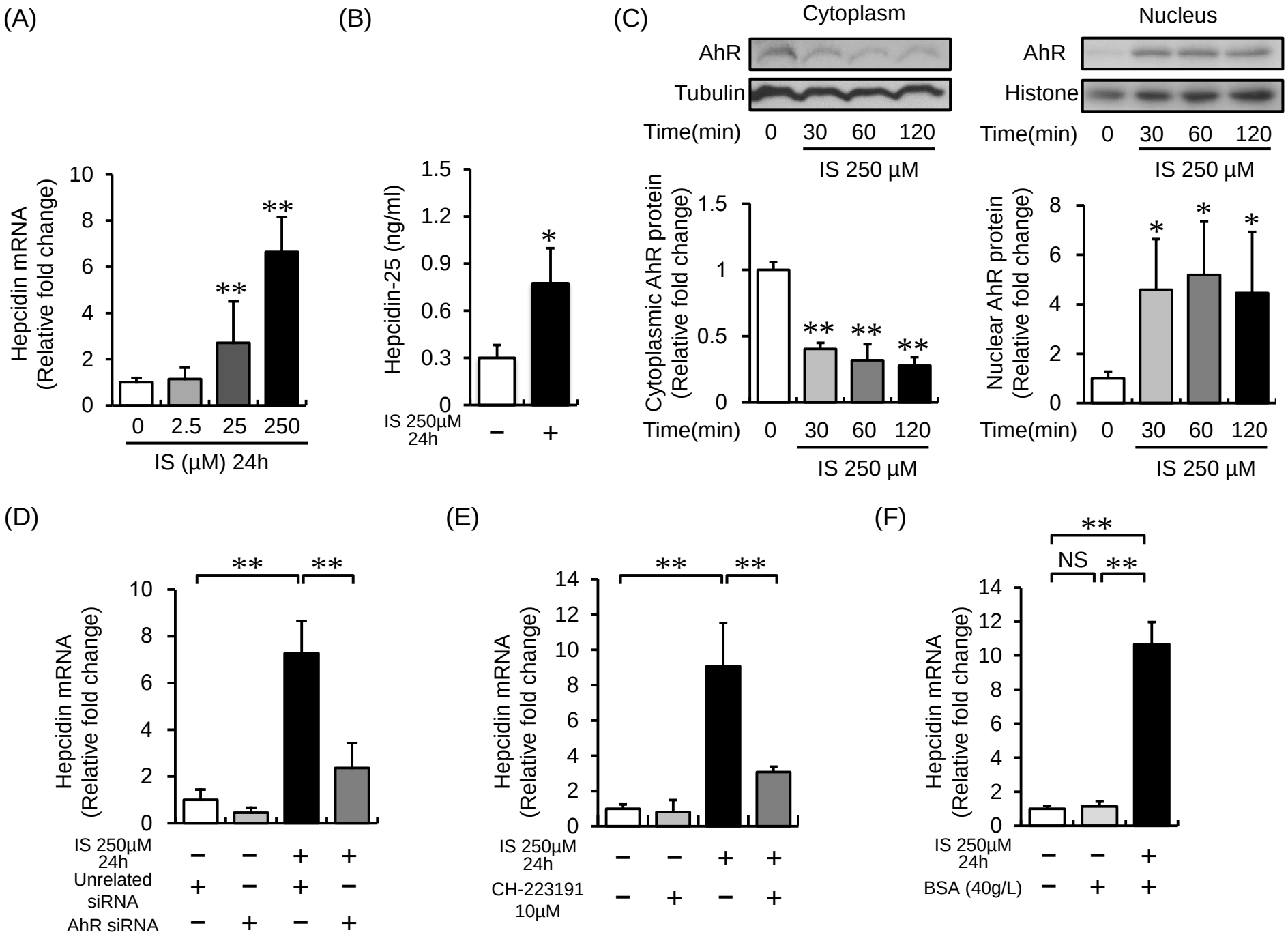

Figure 2 Hamano et al.

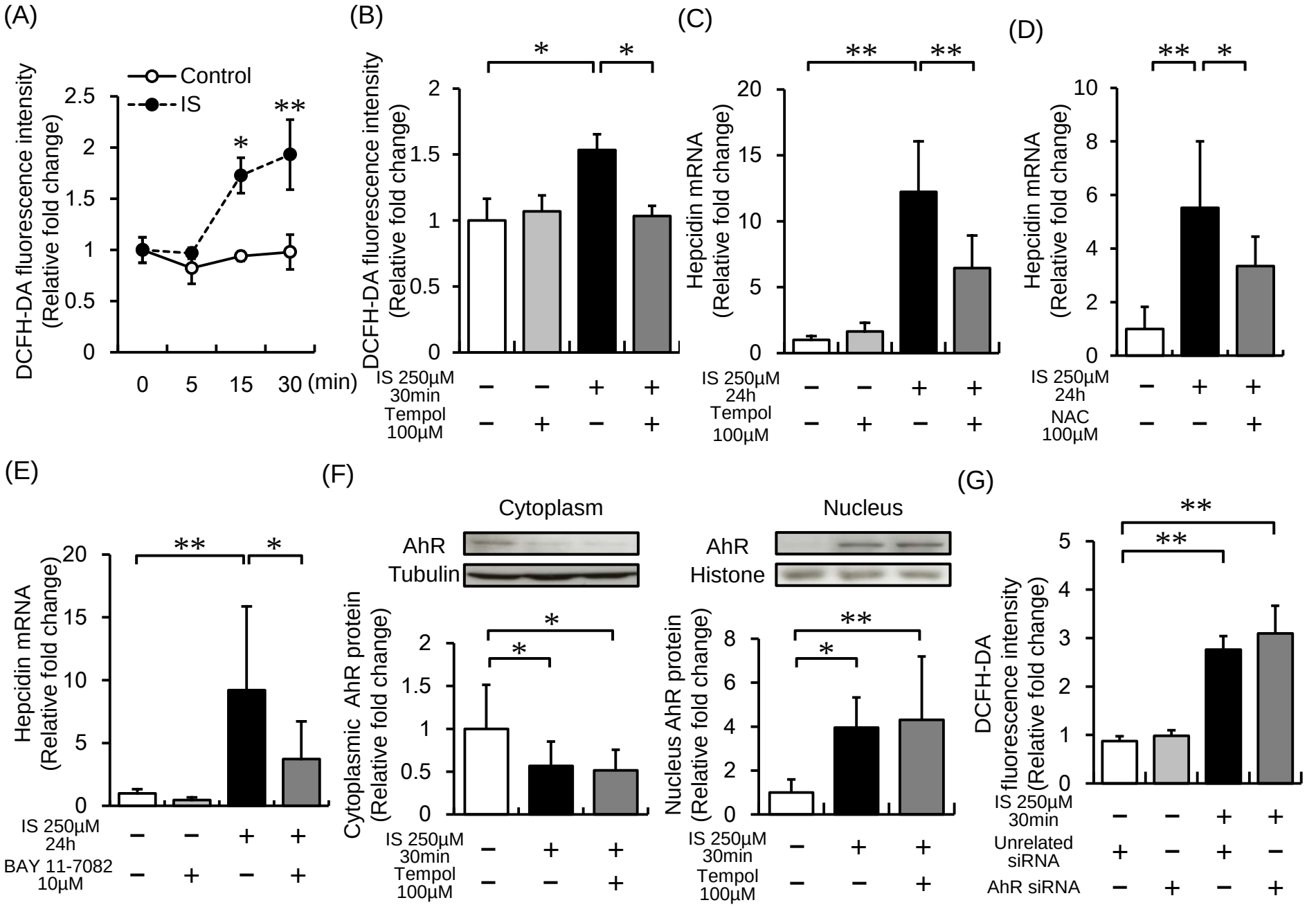

Figure 2 continued

(H)

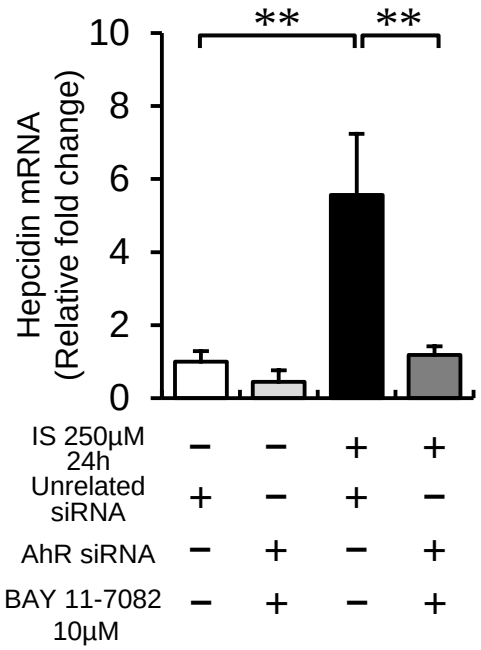

Figure 3 Hamano et al.

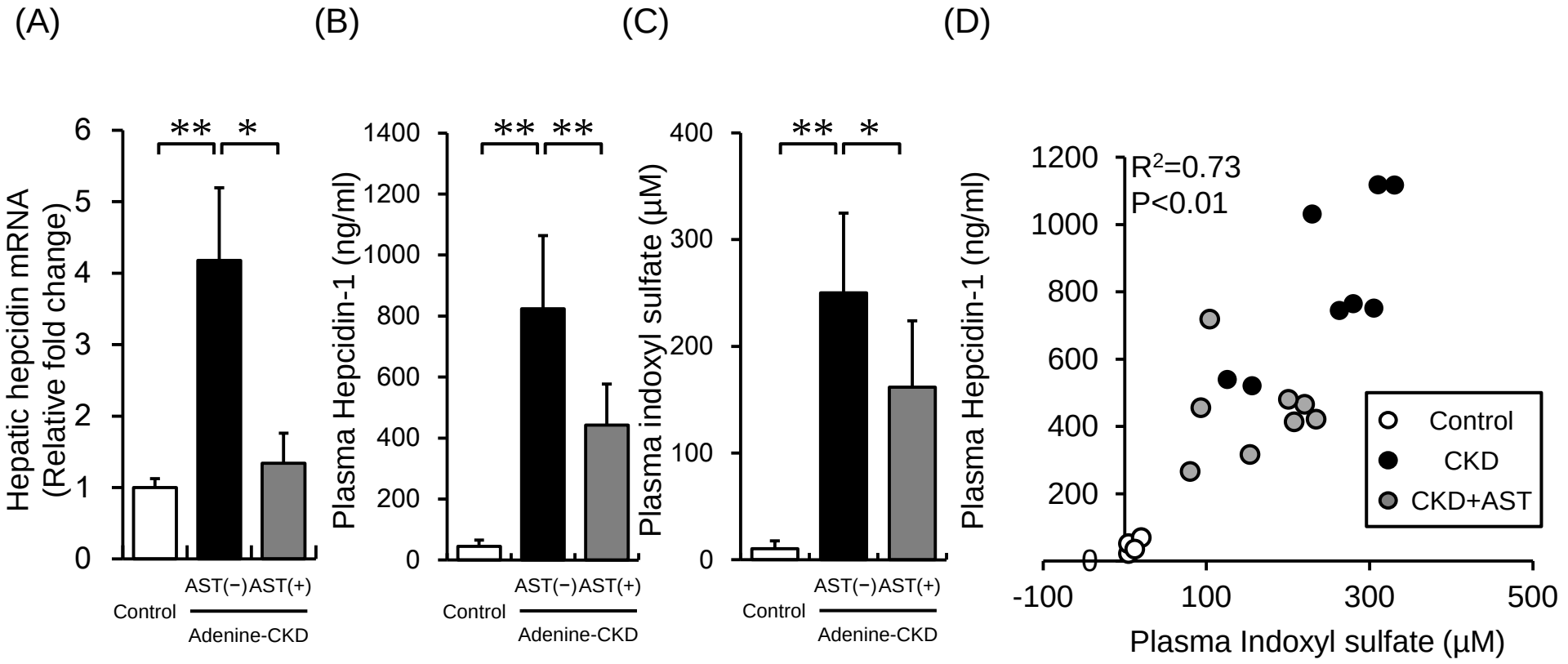

Figure 4 Hamano et al.

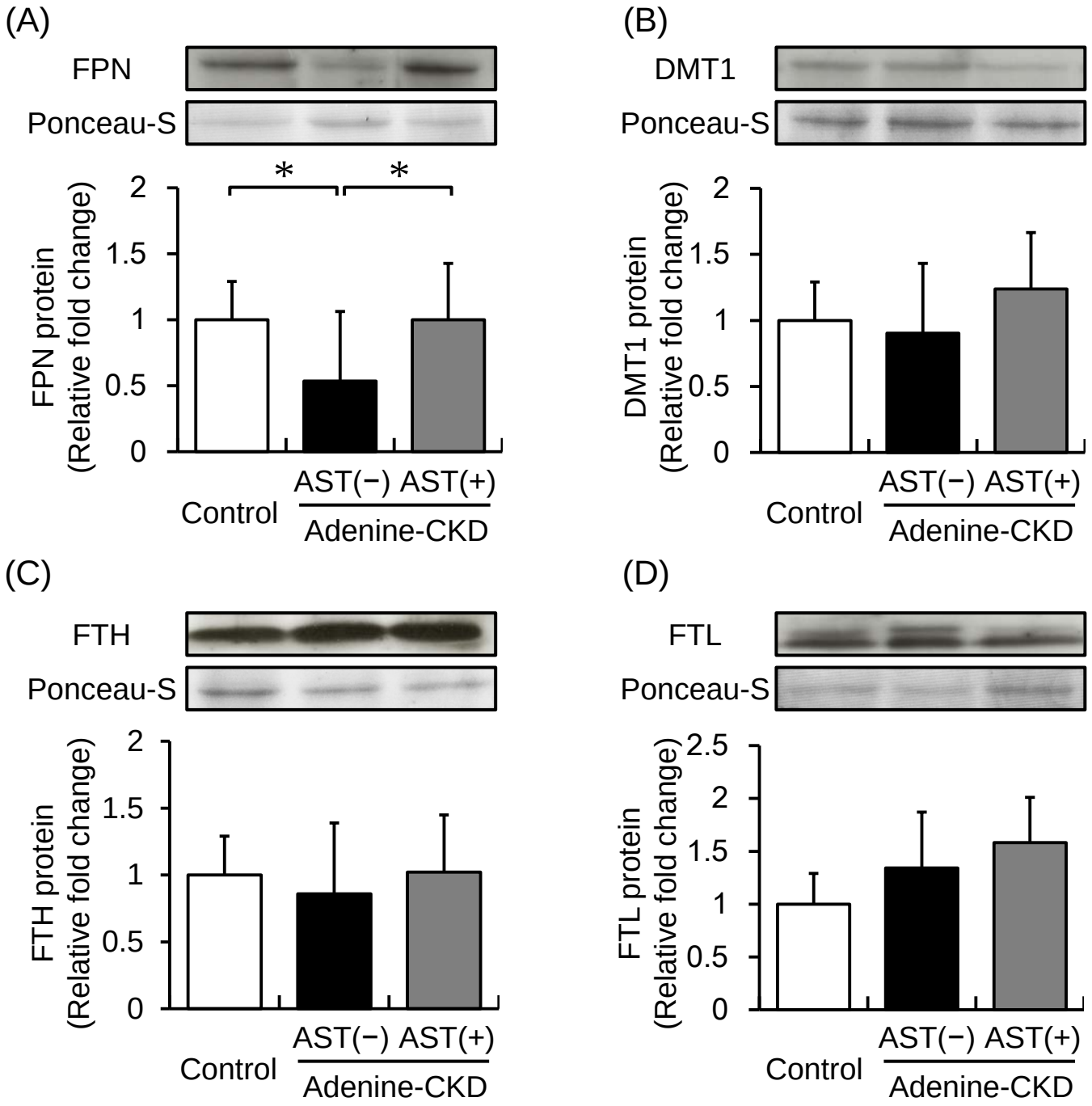

Figure 5 Hamano et al.

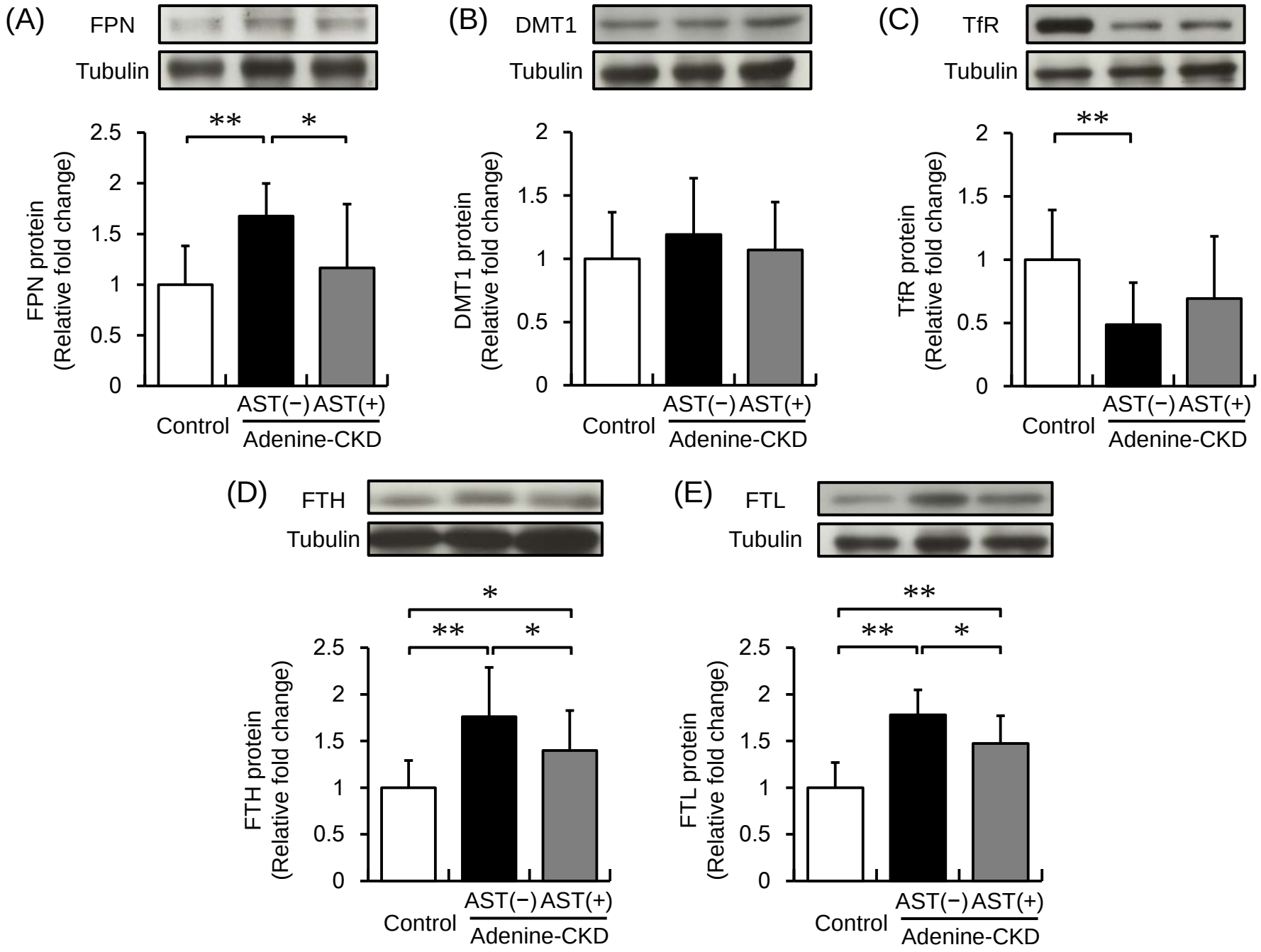

Figure 5 continued

(F)

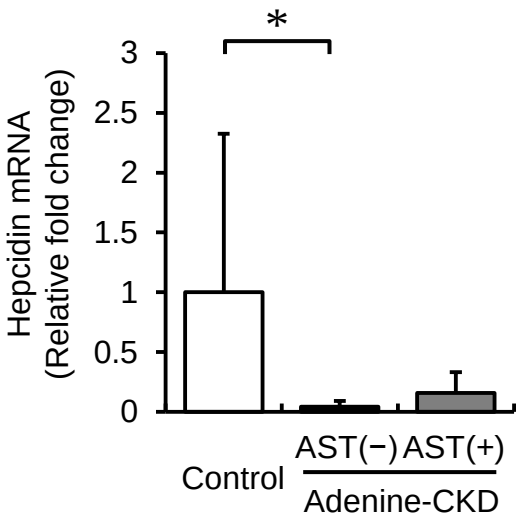

(G)

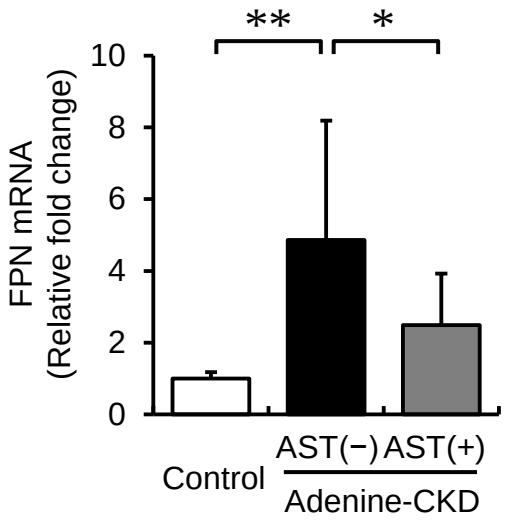

(H)

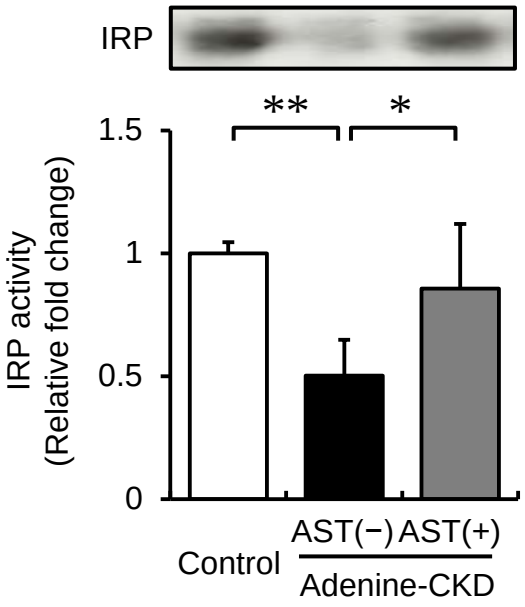

Figure 6 Hamano et al.

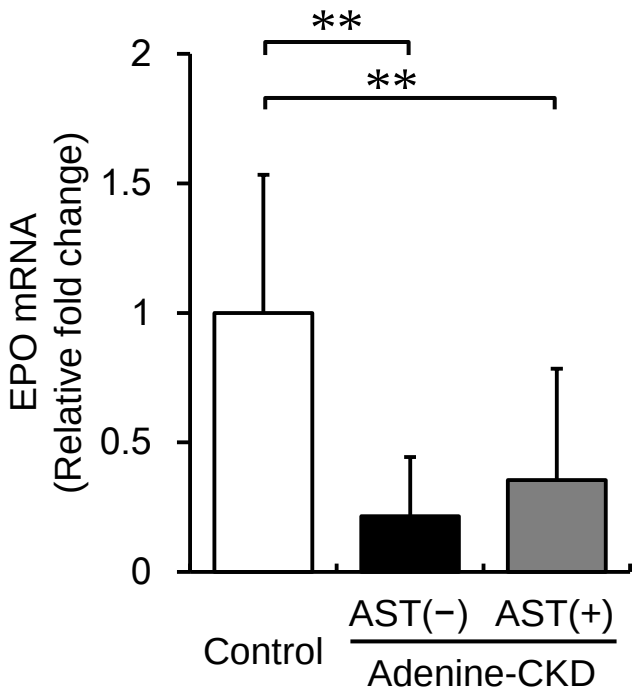

Figure 7 Hamano et al.

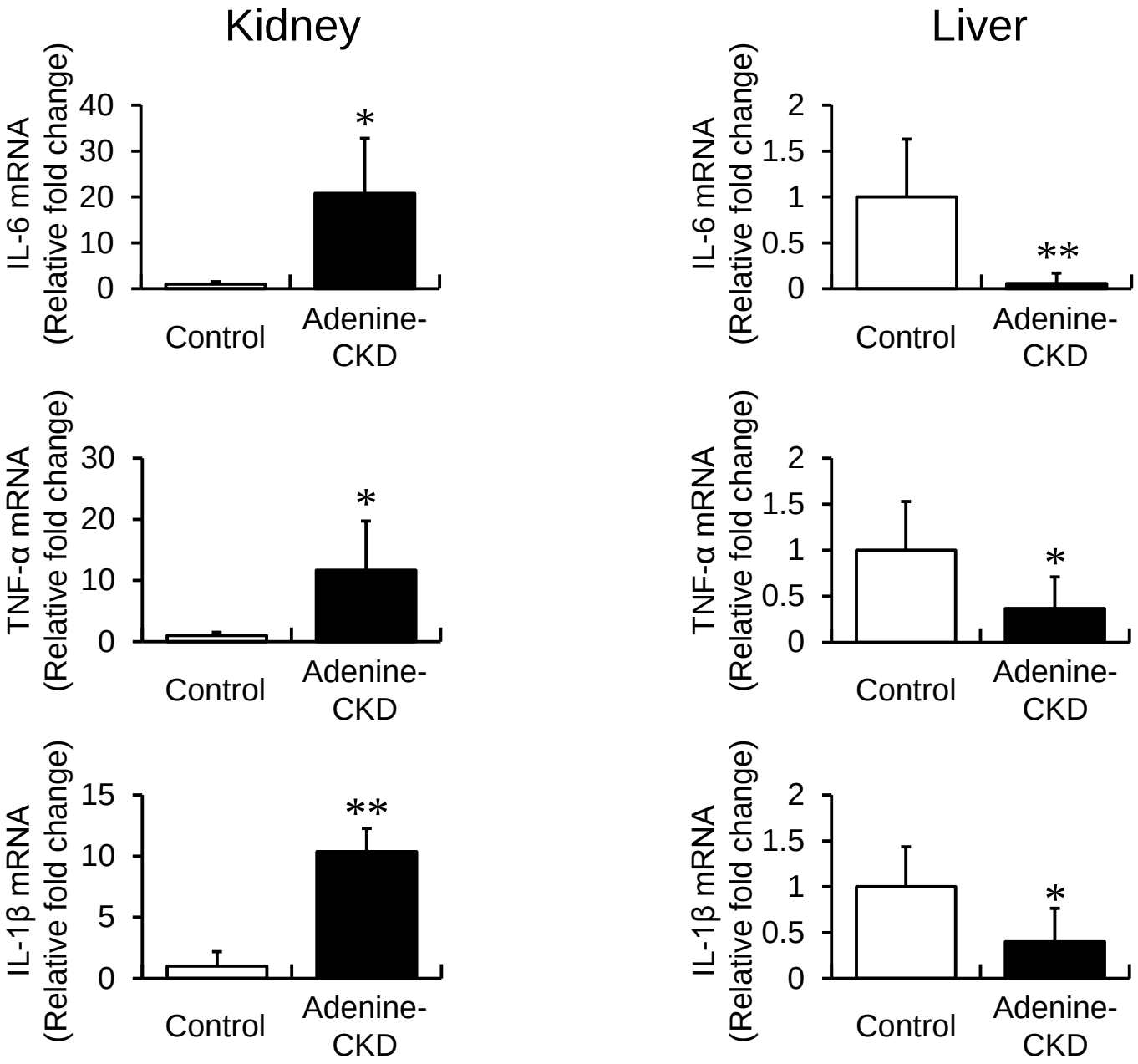

Figure 8 Hamano et al.